This journal is © The Royal Society of Chemistry 2013

SUPPORTING INFORMATION

Silica-supported Ti chloride tetrahydrofuranates, precursors of Ziegler-Natta catalysts

Kalaivani Seenivasan,[a] Erik Gallo,[a,b] Andrea Piovano,[c] Jenny G. Vitillo,[a] Anna Sommazzi,[d] Silvia Bordiga,[a] Carlo Lamberti,[a] Pieter Glatzel,[b] and Elena Groppo*[a]

S1. Experimental - Additional details

X-ray Powder Diffraction

X-ray Powder Diffraction (XRPD) patterns were collected with a PW3050/60 X'Pert PRO MPD diffractometer from PANalytical working in Debye-Scherrer geometry, using as source the high power ceramic tube PW3373/10 LFF with a Cu anode equipped with Ni filter to attenuate K_β and focused by X-ray mirror PW3152/63. Scattered photons were collected by a RTMS (Real Time Multiple Strip) X'celerator detector. The samples were measured as powders inside a 0.8 mm boron-silicate capillary sealed in inert atmosphere.

X-ray Absorption Spectroscopy

X-ray absorption experiments at the Ti K-edge were performed at the BM23 beamline of the ESRF facility (Grenoble, F). The white beam was monochromatized using a Si(111) double crystal; harmonic rejection has been performed by using two silicon mirrors. The intensity of the incident beam was monitored by an ionization chamber (filled with 0.3 bar of N_2 and 1.7 bar of He). The EXAFS spectra of the two reference samples were collected in transmission mode; the beam transmitted through the sample passed further through a second ionization chamber, a Ti foil and a third ionization chamber to ensure the correct energy calibration for any acquisition. Due to Ti dilution (2 wt%), the spectra of Ti^{IV}/SiO_2 and Ti^{III}/SiO_2 were collected in fluorescence mode, by means of a 9 elements germanium monolithic detector. The samples were measured in the form of self-supporting pellets prepared inside the glove-box and placed inside a home-made cell having kapton windows; before measurements, the cell was outgassed in order to remove the Ar, which absorbs most of the beam at this low energy. The two precursors have been diluted in paraffin.

The XANES part of the spectra was acquired with an energy step of 0.3 eV and an integration time of 4 s/point. The EXAFS part of the spectra was collected up to 12 $Å^{-1}$ with a variable sampling step in energy, resulting in $\Delta k = 0.03$ $Å^{-1}$. For each sample, three equivalent EXAFS spectra were acquired and averaged before the data analysis. EXAFS data analysis was performed using the Athena and Arthemis softwares. Phase and amplitudes were calculated by FEFF6.0 code using as input the simple Ti-O and Ti-Cl fragments as determined from the crystal structure of the reference compounds. For each sample, the averaged $k^3\chi(k)$ function was Fourier transformed in the $\Delta k = 2.0\text{-}10.5$ $Å^{-1}$ interval, so that a direct comparison among the different spectra is possible.

The XANES spectra of the two reference compounds were simulated by means of FDMNES code,[1] on clusters having a diameter of 3.0 Å (such as those shown in Figure 4 in the main text) and 8.0 Å. It was found that clusters having a diameter of 3.0 Å are not sufficient to reproduce the experimental spectra, and the dimension of the cluster must be increased up to 8.0 Å.

X-ray Emission Spectroscopy

The vtc-XES experiment was performed at the high brilliance X-ray spectroscopy beamline ID26 at the European Synchrotron Radiation Facility (ESRF, France). The incident energy was selected at 5015 eV (which is above the Ti K-edge at 4966 eV) by means of a pair of cryogenically cooled Si(311) single crystals. Higher harmonics were suppressed by three Si mirrors operating in total reflection. The samples were placed inside an ad hoc in situ cell equipped with kapton windows and oriented at 45° with respect to the incident beam and the X-ray spectrometer crystals. The beam size on the sample was approximately 0.8 mm horizontally and 0.2 mm vertically. The spectrometer exploits the Ge(331) Bragg reflection of five spherically bent analyzer crystals (radius 1000 mm) arranged in a vertical Rowland circle geometry. The emitted photons were detected using an avalanche photo-diode. The resulting total energy resolution was 1.0 eV. All spectra were normalized to the incident flux as monitored by the scattering from a 1 μm silicon nitride foil.

The samples were measured in the form of self-supporting pellets prepared inside the glove-box and placed inside the same home-made cell used for XAS measurements; before measurements, the cell was outgassed in order to remove the Ar, which absorbs most of the beam at this low energy. The two precursors have been diluted in paraffin.

The vtc-XES spectra are superimposed on the $K\beta_{1,3}$ peak tail. The background was subtracted by fitting four Voigt line profiles approximating the $K\beta_{1,3}$. Because of the weak intensity of the vtc-XES lines the subtraction of the background introduces an error in the resulting spectra. To estimate the error the fit procedure was performed using ten different sets of starting values. The fit average was chosen to model the main line tail. [2]

S2. XRPD data

Figure S1 shows the XRPD patterns for of both Ti^{IV}/SiO_2 and Ti^{III}/SiO_2, compared to that of bare silica pre-activated at 550°C. In all the cases, the pattern shows only a broad peak centred around 2θ = 21°, which is assigned to the amorphous silica support.

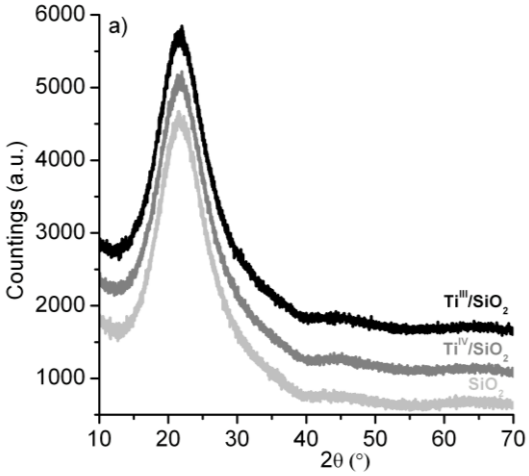

Figure S1. XRPD patterns of Ti^{IV}/SiO_2 and Ti^{III}/SiO_2, compared to that of the SiO_2 support pre-activated at 550°C.

S3. FT-IR spectroscopy: interaction with H_2O

H_2O was chosen as a probe to hydrolyse the silica-supported samples at room temperature, in order to reveal the presence of available surface chlorine. Adsorption of water at room temperature was followed by in situ FT-IR spectroscopy. The FT-IR spectra of H_2O adsorbed on pure SiO_2 (pre-treated at 550 °C), Ti^{IV}/SiO_2 and Ti^{III}/SiO_2 are shown in Figure S2 (the whole 4000 – 1200 cm^{-1} region is shown on the left, whereas a magnification of the ν(OH) region is shown on the right). Black spectra are collected before interaction with H_2O; blue spectra refer to the maximum H_2O coverage (P_{H2O} = 10 mbar), whereas red ones are collected after degassing the samples in dynamic vacuum (*i.e.* correspond to H_2O adsorbed irreversibly). H_2O adsorbed on the bare silica support (Figure S2a) weakly interacts with the surface hydroxyl groups, with the consequent perturbation of the corresponding IR absorption bands; however, no chemical reactions occur on the surface, as testified by the complete reversibility of the adsorbed H_2O. A similar behaviour is observed upon adsorption of water on Ti^{IV}/SiO_2 and Ti^{III}/SiO_2 pre-catalysts (Figure S2c,d); in particular, the formation of new OH species is not observed, testifying that the amount of chlorine is quite low. In contrast, when H_2O is dosed on a similar sample obtained by grafting $TiCl_4$ on pre-treated silica, ($TiCl_4/SiO_2$, Figure S2b) a fast hydrolysis of the exposed Ti-Cl ligands occurs with the attendant formation of new Ti-OH species well visible in the ν(OH) region of the IR spectrum.

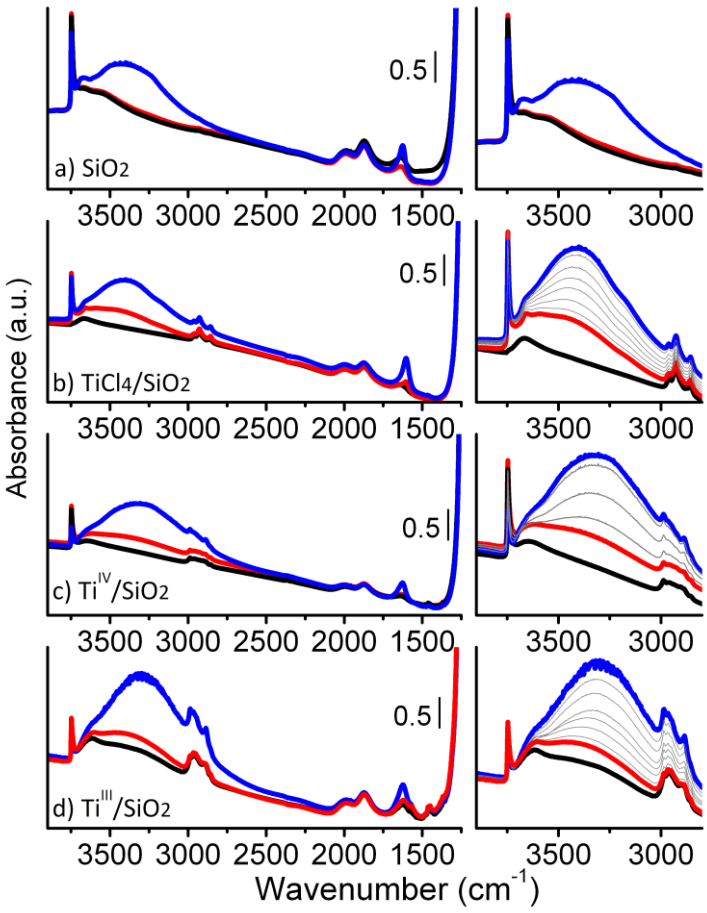

Figure S2. FT-IR spectra of a) SiO_2, b) $TiCl_4/SiO_2$, 2c) Ti^{IV}/SiO_2, and d) Ti^{III}/SiO_2 samples as such (black spectra), in contact with H_2O dosed at room temperature and evolution as a function of the equilibrium pressure (P_{H2O}), from P_{H2O} =10 mbar (blue curve) to P_{H2O} = 10^{-3} mbar (red curve). The whole 4000 – 1200 cm^{-1} region is shown on the left, whereas a magnification of the ν(OH) region is shown on the right.

S4. FT-IR spectroscopy: CO as a probe molecule

The accessibility of the surface Ti species in the Ti^{IV}/SiO_2 and Ti^{III}/SiO_2 samples was investigated by means of FT-IR spectroscopy of CO adsorbed at 100 K. The use of probe molecules is a well known experimental method that allows to determine the properties of the accessible sites at a defined surface.[3-5] It has been demonstrated that CO is able to interact with the Ti sites exposed on well defined surfaces of TiO_2 only at a low temperature.[6-9] The evolution of the FT-IR spectra of CO adsorbed at 100 K on Ti^{IV}/SiO_2 upon decreasing the CO coverage is shown in Figure S3, in the ν(OH) and ν(CO) region, respectively. Similar spectra were obtained for Ti^{III}/SiO_2. In the following, the evolution of the spectra will be discussed from low to high CO coverage. The ν(OH) band at 3748 cm^{-1} due to free silanol groups is gradually consumed upon increasing CO pressure (Figure S3a), accompanied by the appearance of a new band at 3663 cm^{-1} (with a shoulder at 3604 cm^{-1}). The evolution of the spectra in the ν(OH) region is accompanied by the appearance of two IR absorption bands in the ν(CO) region at 2156 and 2137 cm^{-1} (Figure S3b), which are assigned to the vibrational modes of CO adsorbed on the silanol groups and to liquid-like CO, respectively. This behaviour is commonly observed when CO is adsorbed at low temperature on pure silica activated at 550°C. It is important to observe that the strength of CO interaction with the silica surface is very weak, as demonstrated by the persistence of the roto-vibrational profile of gaseous CO also at low CO coverage. In other words, when CO is dosed at 100 K on the Ti^{IV}/SiO_2 and Ti^{III}/SiO_2 samples, no interaction with specific adsorbing sites is observed, but only with the silica surface. In summary, the results of these experiments indicate that, whatever is the state of the Ti sites in Ti^{IV}/SiO_2 and Ti^{III}/SiO_2, they do not have free coordination vacancies available for CO insertion and coordination.

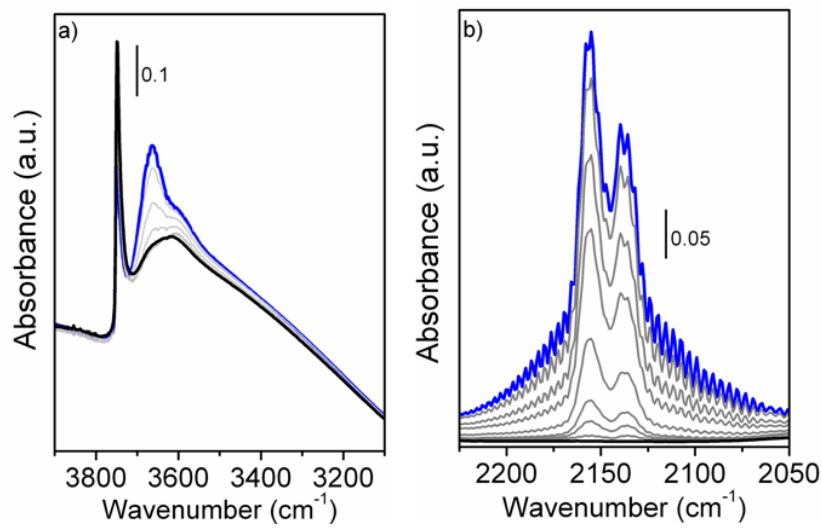

Figure S3. Evolution of the FT-IR spectra of CO adsorbed at 100 K on the Ti^{IV}/SiO_2 sample as a function of CO equilibrium pressure (P_{CO}), from P_{CO} = 40 mbar (blue curve) down to P_{CO} = 10^{-3} mbar (black curve). Part a) shows the ν(OH) region, whereas part b) displays the ν(CO) region, after subtraction of the background (spectrum of the sample before CO dosage).

S5. EXAFS data analysis

In the analysis of the EXAFS data for Ti^{IV}/SiO_2 and Ti^{III}/SiO_2 samples, it was considered that three different ligands can constitute the first coordination sphere around the absorbing Ti atom: oxygen belonging to silica, oxygen belonging to thf ligands, and chlorine. All of them contribute in the same R range. The number of fitting variables is very large and they strongly correlate each others; moreover, the available Δk range is quite short (Δk = 2.0 – 10.5 $Å^{-1}$). For this reason, it was not possible to perform a standard fit, leaving free all the fitting parameters, and the following choices were made:

i) Any trial to fit independently the two oxygen ligands failed. Therefore, a single type of oxygen was included, being aware that any heterogeneity in the Ti-O distance would be accounted for by the Debye-Waller factor (*i.e.* too small Debye-Waller factors for the oxygen contributions are not realistic);

ii) Both Ti-O and Ti-Cl coordination numbers (S_0^2xN) were kept fix to defined values. A series of fit were performed by changing in a systematic way the coordination numbers.

The results of the fits are summarized in Table S1 and Table S2 for Ti^{IV}/SiO_2 and Ti^{III}/SiO_2, respectively.

Table S1. Optimized parameters in the EXAFS analysis for Ti^{IV}/SiO_2. The fit were performed in the R space (ΔR = 1.0 – 3.0 Å) on $k^3\chi(k)$ functions Fourier-Transformed in the 2.0–10.5 $Å^{-1}$ range. The coordination numbers S_0^2xN were not optimized. Non physical values are indicated by an asterisks.

Number and type of ligands[1]	ΔE (eV)	d(Ti-O) (Å)	σ^2(Ti-O) ($Å^2$)	d(Ti-Cl) (Å)	σ^2(Ti-Cl) ($Å^2$)	R_{factor}
5O, 1Cl	0 ± 3	1.83 ± 0.02	0.013 ± 0.002	2.32 ± 0.03	0.008 ± 0.003	0.045
4O, 2Cl	0 ± 3	1.82 ± 0.02	0.010 ± 0.001	2.32 ± 0.03	0.017 ± 0.005	0.042
3O, 3Cl	1 ± 3	1.82 ± 0.01	0.007 ± 0.001	2.31 ± 0.04	0.024 ± 0.005 (*)	0.030
5O	-5 ± 7	1.80 ± 0.04	0.011 ± 0.003	-	-	0.122 (*)
4O, 1Cl	0 ± 3	1.83 ± 0.02	0.010 ± 0.001	2.31 ± 0.03	0.009 ± 0.003	0.027
3O, 2Cl	1 ± 2	1.82 ± 0.01	0.007 ± 0.001	2.31 ± 0.03	0.018 ± 0.003	0.022
2O, 3Cl	1 ± 2	1.81 ± 0.01	0.003 ± 0.001(*)	2.28 ± 0.04	0.026 ± 0.004 (*)	0.021

[1] Arbitrarily fixed in the fitting process.

Table S2. Optimized parameters in the EXAFS analysis for Ti^{III}/SiO_2. The fit were performed in the R space (ΔR = 1.0 – 3.0 Å) on $k^3\chi(k)$ functions Fourier-Transformed in the 2.0–10.5 $Å^{-1}$ range. The coordination numbers S_0^2xN were not optimized. Non physical values are indicated by an asterisks.

Number and type of ligands[1]	ΔE (eV)	d(Ti-O) (Å)	σ^2(Ti-O) ($Å^2$)	d(Ti-Cl) (Å)	σ^2(Ti-Cl) ($Å^2$)	R_{factor}
5O, 1Cl	0 ± 3	1.83 ± 0.02	0.016 ± 0.002	2.34 ± 0.01	0.003 ± 0.001 (*)	0.049
4O, 2Cl	1 ± 3	1.83 ± 0.02	0.011 ± 0.00	2.35 ± 0.02	0.010 ± 0.003	0.097 (*)
3O, 3Cl	1 ± 3	1.82 ± 0.03	0.008 ± 0.002	2.35 ± 0.03	0.017 ± 0.005	0.127 (*)
5O	-6 ± 12(*)	1.80 ± 0.06	0.012 ± 0.003	-	-	0.374 (*)
4O, 1Cl	1 ± 2	1.83 ± 0.02	0.012 ± 0.002	2.34 ± 0.01	0.003 ± 0.001 (*)	0.044
3O, 2Cl	1 ± 3	1.82 ± 0.02	0.008 ± 0.002	2.35 ± 0.02	0.011 ± 0.003	0.088
2O, 3Cl	2 ± 3	1.83 ± 0.02	0.004 ± 0.002(*)	2.34 ± 0.04	0.018 ± 0.005	0.126 (*)

[1] Arbitrarily fixed in the fitting process.

Some of the fits are evidently not good, resulting in variables having a non physical meaning (labelled with an asterisk). In both cases, the first peak in the FT is well fitted with oxygen ligands at a

distance of about 1.82 Å; this distance is definitely shorter than that characteristic of thf ligands in the Ti^{IV} and Ti^{III} precursors (that was around 2.11 Å). The second contribution in the FT of the EXAFS signals corresponds to chlorine ligands at an average distance of about 2.32 Å for Ti^{IV}/SiO_2 and slightly longer (2.35 Å) for Ti^{III}/SiO_2: in both cases, the Ti-Cl distance remains similar to that characteristic of the corresponding precursors. However, the analysis of the EXAFS data is not sufficient to determine the number of oxygen and chlorine ligands for both Ti^{IV}/SiO_2 and Ti^{III}/SiO_2. As a matter of fact, different combination of ligands give equally reasonable fitting results. The best fits (in terms of R_{factor}) for Ti^{IV}/SiO_2 are obtained with 4 oxygen and 1 chlorine, or 3 oxygen and 2 chlorine. For Ti^{III}/SiO_2, the best fit is the one with 3 oxygen ligands and 2 chlorine ligands. In both cases, 3 chlorine ligands are too much, but at least one chlorine is necessary to fit the EXAFS data.

S6. vtc-XES data analysis

Table S3 reports the models used to simulate the vtc-XES spectrum of Ti^{IV}/SiO_2 as a function of the titanium coordination numbers. The models were built using GaussView®, starting from the structure of the $TiCl_4(thf)_2$ precursor, in which titanium is surrounded by two thf ligands and four chlorine ligands. Thus, we considered only models having no more than two thf per titanium and no more than four chlorine per titanium. We also investigated the case of titanium bonded to four oxygen from silica, while we did not explore the cases of titanium bonded with five and six oxygen of the silica because less realistic from a chemical point of view. DFT calculations were performed within the one electron approximation using ORCA 2008 code.[10] The structures were optimized at the TPSSh/TZVP/CP(PPP) level of theory. For the convergence of the optimization procedure, we required a variation of the total energy among two consecutive loops below than 0.0005 eV (threshold). Figure S4 reports as an example the case of model p7. We tested that the energy minimum was a global minimum by performing further twenty-five optimization cycles using 0.0002 eV as total energy threshold.

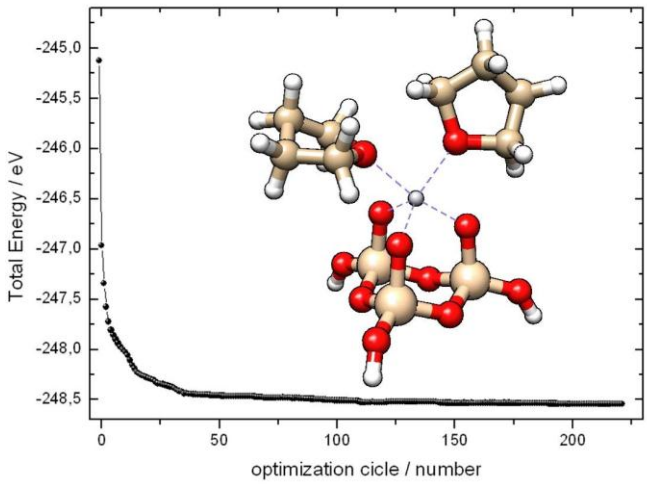

Figure S4. Optimization steps vs Total Energy in the case of model p7.

In order to evaluate the agreement between the simulated and the experimental vtc-XES spectra we have shifted the zero of the energy to the maximum of the Kβ" characteristic of oxygen ligands. We have then fitted the experimental (exp) and theoretical (th) vtc-XES as reported in Ref.[2]. For each peak we have defined the centre of gravity γ as:

$$\gamma = \frac{\sum_i E_i \cdot I_i}{\sum_i I_i}$$

where E_i and I_i are respectively the energy and the intensity of the point i of the fitted peak. The relative agreement (θ) of a cluster model respects to the peak (P) of the experimental spectrum was calculated as:

$$\theta_P = \frac{\gamma_{exp} - \gamma_{th}}{\gamma_{exp}}$$

The global relative agreement of a model Θ was defined as:

$$\Theta = \Pi_{P=A}^{E} \theta_P$$

Small Θ values correspond to a good agreement between theoretical and experimental data. In some theoretical (experimental) data some of the experimental (theoretical) lines are missing. In this case we used as θ_P the worst value among the others determined θ_P.

Table S3. Complete list of all the models employed for simulating the vtc-XES spectrum of Ti^{IV}/SiO_2, as a function of the Ti coordination numbers (f = four-fold, p=penta- and s=six-fold). The relative agreement between the experimental XES spectrum and the theoretical one is reported in terms of the figure of merit Θ. Θ has been normalized to the best value that we obtained. In bold the models giving Θ values below 1.5; both the models and the simulated spectra are shown in Figure 4 of the main text.

Model	O_{SiO2}	O_{thf}	Cl	Θ
f1	1	2	1	1.93
f2	1	1	2	1.81
f3	1	0	3	2.12
f4	2	2	0	1.73
f5	2	1	1	1.63
f6	2	0	2	1.85
f7	3	1	0	2.16
f8	3	0	1	1.98
f9	4	0	0	2.84
p1	1	2	2	1.77
p2	1	1	3	2.51
p3	1	0	4	4.02
p4	**2**	**2**	**1**	**1.39**
p5	**2**	**1**	**2**	**1.46**
p6	2	0	3	1.79
p7	3	2	0	1.67
p8	3	1	1	2.37
p9	3	0	2	2.17
p10	4	1	0	3.07
p11	4	0	1	3.91
s1	1	2	3	2.64
s2	1	1	4	3.28
s3	**2**	**2**	**2**	**1.21**
s4	2	1	3	1.52
s5	2	0	4	2.14
s6	**3**	**2**	**1**	**1.00**
s7	**3**	**1**	**2**	**1.30**
s8	3	0	3	3.88
s9	4	1	1	2.06
s10	4	2	0	2.46
s11	4	0	2	2.23

References

[1] Y. Joly, *Phys. Rev. B* 2001, *63*, art. no. 125120.
[2] E. Gallo, C. Lamberti, P. Glatzel, *Phys. Chem. Chem. Phys.* 2011, *13*, 19409-19419.
[3] A. Zecchina, D. Scarano, S. Bordiga, G. Spoto, C. Lamberti, *Adv. Catal.* 2001, *46*, 265-397 and references therein.
[4] C. Lamberti, E. Groppo, G. Spoto, S. Bordiga, A. Zecchina, *Adv. Catal.* 2007, *51*, 1-74.
[5] C. Lamberti, A. Zecchina, E. Groppo, S. Bordiga, *Chem. Soc. Rev.* 2010, *39*, 4951–5001.
[6] C. Deiana, E. Fois, S. Coluccia, G. Martra, *J. Phys. Chem. C* 2010, *114*, 21531-21538.
[7] K. Hadjiivanov, J. Lamotte, J. C. Lavalley, *Langmuir* 1997, *13*, 3374-3381.
[8] K. Hadjiivanov, B. M. Reddy, H. Knozinger, *Appl. Catal. A-Gen.* 1999, *188*, 355-360.
[9] L. Mino, A. M. Ferrari, V. Lacivita, G. Spoto, S. Bordiga, A. Zecchina, *J. Phys. Chem. C* 2011, *115*, 7694-7700.
[10] F. Neese, *Wiley Interdiscip. Rev.-Comput. Mol. Sci.* 2012, *2*, 73-78.